

# Transferrin Modified Graphene Oxide for Glioma-Targeted Drug Delivery: In Vitro and in Vivo Evaluations

Guodong Liu,<sup>†,#</sup> He Shen,<sup>‡,||,∇,#</sup> Jinning Mao,<sup>§,#</sup> Liming Zhang,<sup>‡</sup> Zhen Jiang,<sup>⊥</sup> Tao Sun,<sup>¶</sup> Qing Lan,<sup>\*,†</sup> and Zhijun Zhang<sup>\*,‡</sup>

<sup>†</sup>Neurosurgery Department, The Second Affiliated Hospital of Soochow University, 1055 Sanxiang Road, Suzhou, 215004, China

<sup>‡</sup>Suzhou Key Laboratory of Nanobiomedicine, Division of Nanobiomedicine, Suzhou Institute of Nano-tech and Nano-bionics, Chinese Academy of Sciences, 398 Ruoshui Road, Suzhou, 215123, China

<sup>§</sup>Cardiovascular Department, The Second Affiliated Hospital of Soochow University, 1055 Sanxiang Road, Suzhou, 215004, China

<sup>⊥</sup>Radiology Department, The Second Affiliated Hospital of Soochow University, 1055 Sanxiang Road, Suzhou, 215004, China

<sup>¶</sup>Department of Biological Sciences, Xi'an Jiaotong-Liverpool University, 111 Ren'ai Road, Suzhou, 215123, China

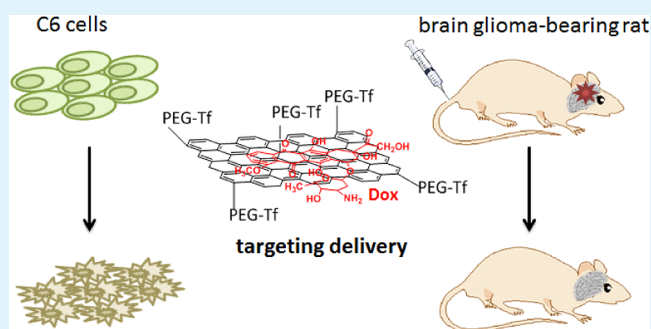
<sup>||</sup>Graduate University of Chinese Academy of Sciences, 19(A) Yuquan Road, Beijing, 100039, China

<sup>∇</sup>Institute of Chemistry, Chinese Academy of Sciences, Zhong Guan Cun Bei Yi Jie 2, Beijing, 100190, China

## S Supporting Information

**ABSTRACT:** Transferrin (Tf), an iron-transporting serum glycoprotein that binds to receptors overexpressed at the surface of glioma cells, was chosen as the ligand to develop Tf-conjugated PEGylated nanoscaled graphene oxide (GO) for loading and glioma targeting delivery of anticancer drug doxorubicin (Dox) (Tf-PEG-GO-Dox). Tf-GO with lateral dimensions of 100–400 nm exhibited a Dox loading ratio up to 115.4%. Compared with Dox-loaded PEGylated GO (PEG-GO-Dox) and free Dox, Tf-PEG-GO-Dox displayed greater intracellular delivery efficiency and stronger cytotoxicity against C6 glioma cells. A competition test showed that Tf was essential to glioma targeting in vitro. The HPLC assay for Dox concentration in tumor tissue and contrapart tissue of the brain demonstrated that Tf-PEG-GO-Dox could deliver more Dox into tumor in vivo. The life span of tumor bearing rats after the administration of Tf-PEG-GO-Dox was extended significantly compared to the rats treated with saline, Dox, and PEG-GO-Dox. In conclusion, we developed Tf-PEG-GO-Dox which exhibited significantly improved therapeutic efficacy for glioma both in vitro and in vivo.

**KEYWORDS:** graphene oxide, transferrin, doxorubicin, glioma, chemotherapy, in vivo



## INTRODUCTION

Gliomas are the most common primary malignant brain tumor and account for about 40% of the incidence. Despite the development of invasive surgery, radiotherapy, and chemotherapy, median survival of patients with glioma has increased little during the past decades.<sup>1,2</sup> It is impossible to thoroughly eradicate glioma by surgery for infiltration growth. Furthermore, blood brain barrier (BBB) restricts the penetration of drugs systemically administrated to glioma.<sup>3</sup> Traditional strategies to overcome BBB include intracerebral injection or infusion of hyperosmotic solutions such as mannitol.<sup>4</sup> These approaches can increase intracranial drug levels but impose higher risk for patients. Nanoparticles have been regarded as a potential alternative to pass through BBB and guide targeted therapy so that individual cancer cells can be destroyed by the loaded agents without causing diffuse damage to surrounding brain tissues.<sup>5,6</sup> An approach for targeting nanoparticles to tumor is to functionalize their surface with ligands such as

transferrin (Tf). Tf is a monomeric glycoprotein that can transport one (monoferric Tf) or two (diferric Tf) iron atoms.<sup>7</sup> Transferrin receptor (TfR) is overexpressed on the brain capillary endothelium and surface of glioma cells, but its level is very low in normal tissues.<sup>8,9</sup> Tf-mediated transcytosis has been demonstrated to transport across BBB, and Tf coupled nanocarriers have potential for glioma targeting therapy.<sup>5,10–13</sup>

Graphene is a two-dimensional nanomaterial widely investigated for its applications in many fields.<sup>14–17</sup> Graphene oxide (GO) is an important derivative of graphene, and its good biocompatibility and lack of obvious toxicity make it a promising drug carrier.<sup>18,19</sup> However, most of the studies with GO have focused on the delivery of antitumor drugs in vitro.<sup>20–23</sup> Doxorubicin (Dox) is a widely used chemotherapy

Received: January 13, 2013

Accepted: July 12, 2013

Published: July 12, 2013

agent, but it can hardly pass through BBB, which limited its clinical utility on glioma. Dox can be loaded onto GO via simple  $\pi$ - $\pi$  stacking with high efficiency.<sup>22,23</sup> Therefore, a GO-based nanocarrier loading Dox for glioma targeting was designed in this study. Tf was chemically conjugated to the surfaces of GO (Figure 1), onto which Dox was then adsorbed.

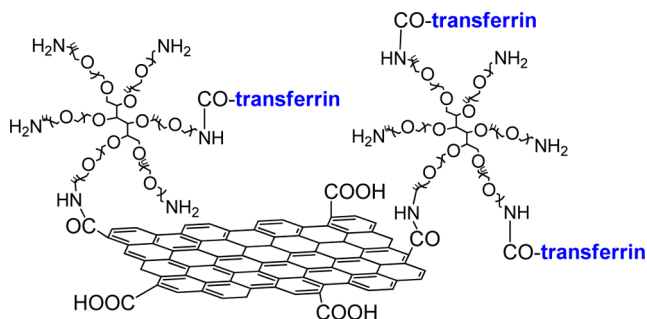


**Figure 1.** Schematic drawing of Tf-PEG-GO conjugate.

The antitumor efficacy of Tf-conjugated PEGylated nanoscaled graphene oxide (GO) for loading and glioma targeting delivery of anticancer drug doxorubicin (Dox) (Tf-PEG-GO-Dox) was evaluated using C6 glioma cells and glioma-bearing rats via systemic administration.

## EXPERIMENTAL SECTION

**Materials and Instrumentation.** Transferrin (Tf) and 3-(4,5-dimethylthiazol-2-yl)-2,5-diphenyltetrazolium bromide (MTT) were obtained from Sigma-Aldrich. Doxorubicin (Dox) was bought from Beijing Huafeng United Technology Co., China. Bicinchoninic acid (BCA) protein assay kit was purchased from Shenergy Biocolor Bioscience and Technology. Native graphite flake and 1-ethyl-3-(3-dimethylaminopropyl) carbodiimide (EDC) were purchased from Alfa Aesar. 6-arm polyethylene glycol-amine (MW: 10 KDa) was obtained from Sunbio Inc. Other chemicals of analytical grade were acquired from China National Medicine Corporation. Milli-Q water was used in all experiments. UV-vis spectra were collected with a Shimadzu UV-2550 spectrophotometer. Morphology of Tf-PEG-GO was characterized by an atomic force microscope (AFM) (Veeco Dimension 3100 atomic force). Dox concentration was determined via HPLC (waters1525, USA). C6 cell line was kindly provided by Dr. Liemei Guo, Shanghai Jiaotong University. Cell culture medium and fetal bovine serum (FBS) were ordered from Invitrogen (Gibco, Carlsbad, CA). Sprague-Dawley rats (weight 200–250 g) were obtained from Laboratory Animals Center of Soochow University. The animals used for the experiments were treated according to protocols approved by Ethical Committee of Soochow University.

**Synthesis of Tf-PEG-GO.** GO was prepared by modified Hummers method<sup>22,24</sup> and converted to carboxylated GO, followed by PEGylation as described in our previously work.<sup>22,25</sup> The glioma targeting drug delivery system, Tf-PEG-GO, was developed via coupling of Tf to PEG-GO by EDC chemistry. Briefly, Tf was dissolved at 1 mg/mL in 50 mM MES buffer by sonicating for 5 min. Then, 5 mM NHS aqueous solution was added to the protein solution and reacted for 15 min at room temperature. EDC was added quickly (the final concentration of EDC was 2 mg/mL) and then continually stirred for 1 h. The suspension was filtered and rinsed thoroughly with distilled water to remove excess agent. Next, 5 mL of PEG-GO solution (1 mg/mL) was added to the above suspension and kept for 4 h. The final product was washed thoroughly to remove unbound protein. The concentration of conjugated protein was determined using a BCA protein assay kit.

**Loading of Dox.** Loading of Dox onto the GO sheets was carried out by adding 2 mL of Dox (2 mg/mL dissolved in DMSO) to 2 mL of Tf-PEG-GO or PEG-GO aqueous suspension with stirring for 12 h

under the darkness. The final product was filtered (MWCO: 10 kDa) against distilled water to remove the free drug. The loading ratio of Dox was estimated by UV-vis spectra, after subtracting the absorbance at 481 nm from GO.

**Cytotoxicity and Competition Assay.** C6 glioma cells were seeded into 96-well culture plates at a density of  $5 \times 10^4$  cells/well and maintained in 100  $\mu$ L of DMEM medium supplemented with 10% FBS in an environmental chamber at 37 °C in 5% CO<sub>2</sub> for 24 h. Free Dox, Dox-loaded PEGylated GO (PEG-GO-Dox), and Tf-PEG-GO-Dox were dissolved in 100  $\mu$ L of culture medium, respectively, and then added into each well. The final concentration of Dox in the medium was kept in the range of 0–80  $\mu$ g/mL. Five wells treated only with culture medium were used as blank controls. The cytotoxicity was measured 24 h later by the MTT assay, and the absorbance was read on a microplate reader at 540 nm. The survival percentages were calculated as: Survival % = ( $A_{540 \text{ nm}}$  for the treated cells/ $A_{540 \text{ nm}}$  for the control cells)  $\times$  100%. Each assay was conducted in triplicate. Finally, concentration–viability curves were made and IC50 values were calculated. Similarly, cytotoxicity of PEG-GO and Tf-PEG-GO on C6 glioma cells was evaluated. In all experiments, the final concentration of GO was adjusted to range from 0 to 800  $\mu$ g/mL.

In the competition assay, C6 glioma cells were seeded into 96-well culture plates as above and then pretreated with an excessive amount of Tf (50  $\mu$ g) dissolved in 100  $\mu$ L of culture medium for 30 min; the supernatant was removed and washed twice with ice cold PBS. Next, Dox, PEG-GO-Dox, or Tf-PEG-GO-Dox was added into each well. The MTT assay was performed to evaluate the cytotoxicity. Each assay was repeated 3 times; concentration–viability curves were then obtained, and IC50 was calculated.

**C6 Glioma Cellular Uptake.** C6 cells were seeded into 24-well plates at a density of  $2 \times 10^6$  cells/well, culturing for 24 h for cell attachment; then, free Dox, PEG-GO-Dox, and Tf-PEG-GO-Dox was added with the final Dox concentration of 3  $\mu$ g/mL in each well. Afterward, the plates were incubated at 37 °C for 1, 2, 4, 8, and 12 h, respectively. At each time point, the cells were washed twice with PBS and further incubated with 0.4 mL of 1% Triton X-100 at 4 °C for 12 h. Twenty-five  $\mu$ L of cell lysate from each well was then collected to estimate the total cell protein content. The rest of the cell lysate was collected for HPLC assay of Dox concentration as described previously with 3 times repeating.<sup>12,26</sup> The cellular uptake index (UI) was calculated according to the following equation:

$$\text{UI} = \text{Dox } (\mu\text{g}) / \text{cellular protein (mg)}$$

**Tissue Distribution Assay.** The brain glioma-bearing rat model was established with stereotactic injection of  $5 \times 10^6$  C6 cells into the right striatum of adult male Sprague-Dawley rats weighing between 200 and 250 g.<sup>27</sup> For the tissue distribution assay, 9 rats were equally and randomly divided into 3 groups after tumor implantation for 10 days. Three hours after intravenous administration of free Dox, PEG-GO-Dox, or Tf-PEG-GO-Dox (dose of Dox 3 mg/kg), the rats were sacrificed and the brain tissues and major organs including liver, spleen, kidney, lung, and heart were excised and washed by cold PBS to remove surface blood. Left striatum (normal brain tissue) and right striatum (tumor tissue) was separated from the brain tissue. HPLC analysis was performed to determine Dox concentration in biological samples.<sup>12</sup>

**Tumor Volume Inhibition and Survival Curves.** 52 glioma bearing rats were randomly and equally divided into 4 groups, on the seventh day of post-intracranial implantation. The rats in the control group were treated with physiological saline. The animals in the other 3 groups were administered free Dox, PEG-GO-Dox, or Tf-PEG-GO-Dox, respectively, through the tail vein at a dose of 2 mg/kg Dox. The treatment was performed every 2 days with a total of 3 doses per rat. On the 14th day of post-tumor implantation, 3 rats of each group were sacrificed randomly, and the brain tissue was extracted and fixed by 4% formaldehyde solution overnight; tumors were completely excised, and the tumor volume was calculated using the following equation:

$$\text{volume (mm}^3\text{)} = l \text{ (mm)} \times w \text{ (mm)} \times h \text{ (mm)}$$

where  $l$  refers to the major anteroposterior diameter,  $w$  is the major diameter from left to right, and  $h$  stands for the major diameter from top to bottom.  $l$ ,  $w$ , and  $h$  values were measured by a vernier caliper.<sup>27</sup> The other 10 rats in each group were maintained to monitor their life span and analyzed by the Kaplan–Meier survival curves.<sup>12,27</sup>

**Statistics.** Significance among groups was determined by one way analysis of variance (ANOVA), and multigroup comparisons were made by the post hoc test. Survival data were presented in Kaplan–Meier curves and analyzed with a log-rank test. Differences were considered significant at  $p < 0.05$ .

## RESULTS AND DISCUSSION

### Synthesis and Characterization of the Nanomaterials.

GO was obtained by oxidation of graphite following the

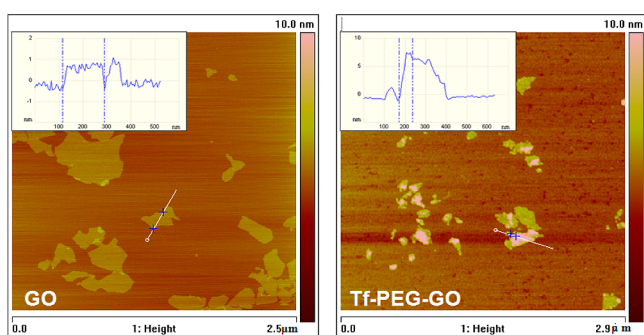


Figure 2. AFM images of GO and Tf-PEG-GO.

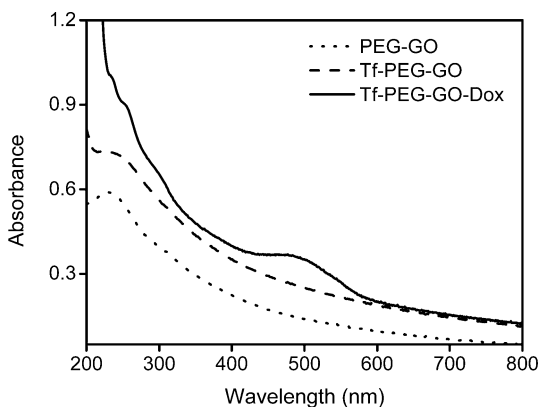


Figure 3. UV–vis spectra of PEG-GO and Tf-PEG-GO before and after being loaded with Dox.

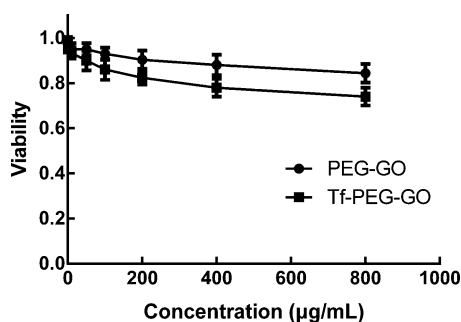


Figure 4. C6 viability–concentration curves for PEG-GO and Tf-PEG-GO.

modified Hummers method and then modified with amine-terminated 6-armed PEG to improve the biocompatibility and enhance blood circulation of graphene.<sup>24,25,28</sup> PEG-GO was

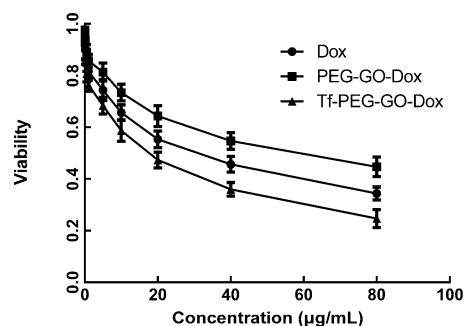


Figure 5. C6 viability–concentration curves for Dox, PEG-GO-Dox, and Tf-PEG-GO-Dox.

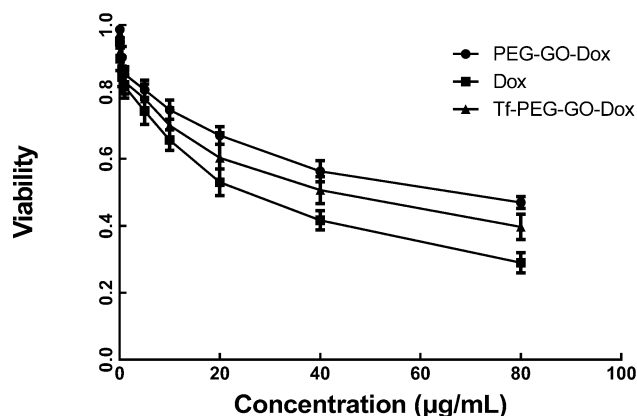


Figure 6. C6 viability–concentration curves for Dox, PEG-GO-Dox, and Tf-PEG-GO-Dox with 50  $\mu\text{g}$  of Tf in each well, added in advance.

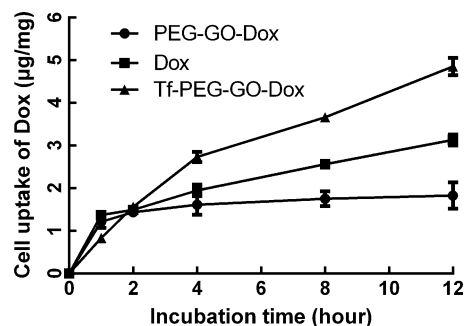


Figure 7. C6 cell uptake of different formulations (Dox concentration, 3  $\mu\text{g}/\text{mL}$ ) at 37  $^{\circ}\text{C}$  from 1 to 12 h.

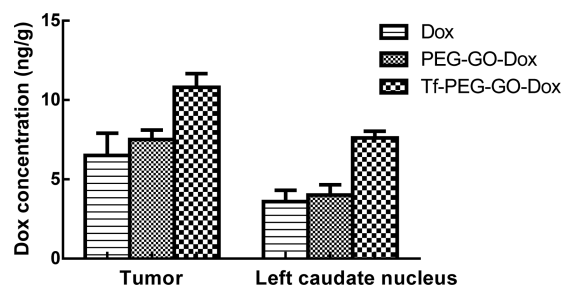
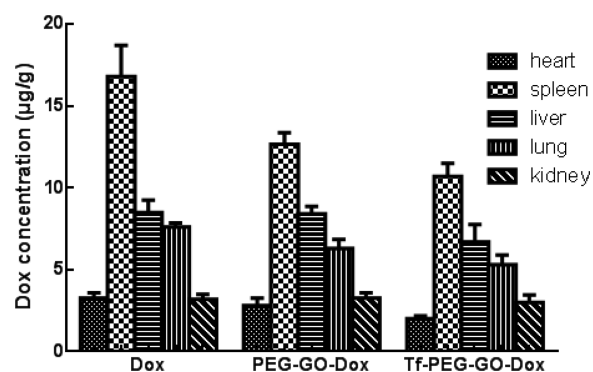
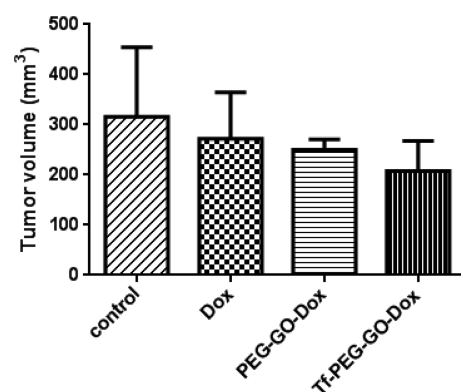


Figure 8. Distribution of Dox in the tumor and left caudate nucleus in brain, after i.v. of Dox, PEG-GO-Dox, and Tf-PEG-GO-Dox ( $n = 3$ ).

highly stable in physiological solutions. PEG-GO was subsequently covalently functionalized with Tf (77 KDa) in the presence of NHS and EDC (Figure 1) because Tf is a classic ligand targeting both the BBB and tumor.<sup>8,9,13</sup>



**Figure 9.** Distribution of Dox in heart, spleen, liver, lung, and kidney, after i.v. of Dox, PEG-GO-Dox, and Tf-PEG-GO-Dox ( $n = 3$ ).



**Figure 10.** Glioma volume in different therapeutic groups on the 14th day. Data were presented as the mean  $\pm$  SD ( $n = 3$ ).  $p < 0.05$ , Tf-PEG-GO-Dox vs PEG-GO-Dox, free Dox, or control group.

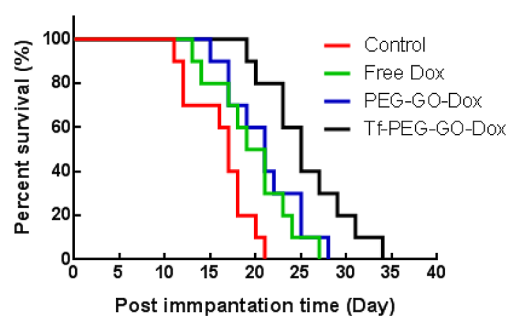


**Figure 11.** Percentage of survival (Kaplan–Meier plot) of glioma bearing rats after i.v. of 2 mg/kg Dox on days 7, 9, and 11 of post-intracranial implantation with different formulations ( $n = 10$ ).

AFM was employed to characterize the morphology of PEG-GO and Tf-PEG-GO (Figure 2). Both GO and Tf-PEG-GO had lateral dimensions of 100–400 nm. While GO was 1–2 nm thick, which was characteristic of a single or two layer sheets,<sup>15</sup>

the thickness of GO was increased to 4–5 nm after conjugation with PEG and transferrin, confirming the formation of Tf-PEG-GO. The concentration of conjugated protein was determined to be 0.17 mg/mL Tf covalently linked with 1 mg/mL PEG-GO. Furthermore, the conjugation prevented GO from the agglomeration in high salt condition. To prolong the circulation time in the body, the nanocarriers should be sufficiently hydrophilic in order to minimize the adsorption of opsonins.<sup>29</sup> Thus, both PEG-GO and Tf-PEG-GO were designed to increase surface hydrophilicity, allowing for low affinity to opsonins and prolonged circulation of the nanocarrier in the blood before reaching the targeted sites. Furthermore, the nanocarriers should be in the appropriate size range. Previous work suggested that the suitable size for nanocarriers to cross the BBB is 100–200 nm in diameter.<sup>5</sup> However, one key feature of glioma is vasculogenesis. The newly formed vessels do not exhibit BBB characteristics. First, vascular density in glioma is much higher than normal brain tissue. Second, the gaps between neovascular endothelial cells in glioma are larger, even up to 0.38  $\mu\text{m}$ . Both factors contribute to the enhanced permeability and retention (EPR) effect of glioma.<sup>30–32</sup> Moreover, glioma can degrade tight junctions by secreting soluble factors, eventually leading to BBB disruption and glioma invasion into brain tissues.<sup>33</sup> Therefore, a leaky vasculature allows the bypassing of the nanocarrier even in the size range of 100 to 400 nm, similar to that of GO used in the present work, which was further confirmed by the tissue distribution assay.

**Loading of Dox.** In our strategy, we chose Dox, a widely used anthracyclinc antibiotic, as a model drug to treat glioma. The anticancer effect of Dox derives from DNA intercalation, the interaction with DNA topoisomerase I and II, reactive oxygen species (ROS) production, and the induction of apoptosis.<sup>34</sup> Dox was loaded onto Tf-PEG-GO via physisorption, mainly in the form of  $\pi$ - $\pi$  stacking and hydrophobic interactions.<sup>22,25</sup> UV-vis spectra were employed to examine the drug loading behavior of Tf-PEG-GO (Figure 3). The characteristic absorption peak of Dox ( $\sim 490$  nm) appeared in the sample of Tf-PEG-GO-Dox, indicating successful formation of Tf-PEG-GO-Dox conjugates. The amount of loaded Dox was estimated by the absorbance at 490 nm, after subtracting the absorbance of GO. In addition, the concentration of Tf-PEG-GO was evaluated by the absorbance at 600 and 800 nm, respectively. The concentrations of Tf-PEG-GO and the loaded Dox were estimated to be 240 and 277  $\mu\text{g/mL}$ , respectively. Therefore, the loading ratio (the weight ratio of loaded drug to carriers) was estimated to be 115.4%, close to that of PEG-GO (127%), indicating efficient loading of Dox by Tf-PEG-GO.

**Cytotoxicity and Competition Assay.** To exclude the possible effects of blank PEG-GO and Tf-PEG-GO on the growth of C6 glioma cells, cytotoxicity of PEG-GO and Tf-PEG-GO was evaluated and no significant toxicity was found

**Table 1. Median Survival Time for Glioma Bearing Rats of Different Therapeutic Groups<sup>a</sup>**

group	median (days)	standard error	95% confidence interval	log-rank test	ISTC (%)	ISTS (%)	ISTG (%)
control	17	0.78	15.48–18.52		–	–	–
free Dox	19	1.58	15.90–22.10	<i>b</i>	11.8	–	–
PEG-GO-Dox	21	1.55	17.96–24.04	<i>b</i>	23.5	10.5	–
Tf-PEG-GO-Dox	25	1.55	21.96–28.04	<i>b, c, d</i>	47.1	31.6	19.0

<sup>a</sup>Dosage of Dox is 3  $\times$  2 mg/kg. Log-rank test vs control. <sup>b</sup> $p < 0.05$  vs saline. <sup>c</sup> $p < 0.05$  vs free Dox. <sup>d</sup> $p < 0.05$  vs PEG-GO-Dox. The increases in survival times (%) are compared to saline (ISTC), to free Dox solution (ISTS), or to PEG-GO-Dox (ISTG).

(Figure 4). Even at the highest concentration (0.8 mg/mL), the cellular viability was above 80%. There were no significant differences in cellular viability between PEG-GO and Tf-PEG-GO ( $p > 0.05$ ). These results demonstrated that PEG-GO had little cytotoxicity, consistent with previous studies.<sup>18,21,23,35</sup> Examination of C6 glioma cell viability showed that the cytotoxicity of Tf-PEG-GO-Dox, PEG-GO-Dox, and Dox were concentration dependent, and their IC50 values (50% glioma inhibition drug concentration) were 13.61, 63.01, and 28.43  $\mu\text{g}/\text{mL}$ , respectively. Clearly, Tf-PEG-GO-Dox exhibits a 4.63 intensification of cell inhibition compared to PEG-GO-Dox ( $p < 0.01$ , Figure 5).

As TfR is overexpressed at the surface of glioblastoma cells, it will compete with Tf-PEG-GO-Dox to bind TfR on the cell surface after adding free Tf into the culture medium. Consequently, less Tf-PEG-GO-Dox could bind TfR and the transportation of Dox was also decreased, leading to the declined cytotoxicity of Tf-PEG-GO-Dox. Thus, in the competition assay, pretreatment with Tf led to markedly decreased cytotoxicity of Tf-PEG-GO-Dox but had no significant effects on the cytotoxicity of GO-Dox or Dox. The IC50 values of Tf-PEG-GO-Dox to C6 glioma cells were increased to 40.16  $\mu\text{g}/\text{mL}$  with Tf pretreatment, compared to that of Tf-PEG-GO-Dox without Tf pretreatment (13.61  $\mu\text{g}/\text{mL}$ ) (Figure 6). These results revealed that the conjugation of Tf to PEG-GO is essential to the pharmacological effect of Tf-PEG-GO-Dox on C6 glioma cells (Figure S1, Supporting Information).

**C6 Glioma Intracellular Uptake.** The targeting efficiency of different formulations was quantitatively assessed by the uptake of C6 glioma cells via HPLC assay. The intracellular Dox level was increased in all groups in a time-dependent manner (Figure 7). In addition, Tf-PEG-GO-Dox could transfer Dox into C6 glioma cells at a faster rate than GO-Dox or Dox. These results are consistent with cytotoxicity data. After incubation for 12 h, the cellular uptake index of Tf-PEG-GO-Dox was much higher than that of PEG-GO-Dox, suggesting that Tf facilitates GO targeting to C6 glioma cells. TfR is overexpressed on the surface of glioma cells.<sup>9</sup> Therefore, the TfR-mediated endocytosis is an efficient cell entry pathway for Tf conjugated nanocarriers.<sup>35,36</sup> After conjugation of Tf to PEG-GO, the transport efficiency of Dox is improved significantly, rendering it a potential nanocarrier for glioma targeting chemotherapy. The cytotoxicity data were analyzed by ANOVA and Bonferroni post hoc test ( $p < 0.05$ ).

**Tissue Distribution Assay.** To further evaluate the therapeutic efficacy of Tf-PEG-GO-Dox to glioma in vivo, C6 glioma-bearing rat model was established and treated with different reagents via systemic administration. Then, brain samples were collected; left striatum (normal brain tissue) and right striatum (tumor tissue) were separated from the brain, and Dox concentration in the two parts was analyzed. In the Tf-PEG-GO-Dox group, Dox concentration in glioma tissue was significantly higher than that in the normal brain tissue (Figure 8), which indicated that Tf-PEG-GO-Dox entered the brain and further accumulated at the tumor site. Moreover, Dox concentration in glioma tissue of the Tf-PEG-GO-Dox group was remarkably higher than that of the other groups, as analyzed by ANOVA and Bonferroni post hoc test ( $p < 0.01$ ), demonstrating that Tf-PEG-GO-Dox can transport more Dox to the tumor site and improve its antitumor effect. In the other 2 groups, Dox concentration in glioma tissue was slightly higher

than the contralateral part of brain ( $p < 0.05$ ), probably due to the EPR effect.

Dox distribution in other tissues displayed that Dox accumulated mostly in both the spleen and the liver. Interestingly, the concentrations of Tf-PEG-GO-Dox and PEG-GO-Dox in the spleen and the liver were significantly lower than that of the free Dox group (Figure 9), clearly indicating that PEGylated GO loaded with Dox enhanced the circulation time and reduced the accumulation of GO in the spleen or liver. Both Tf-PEG-GO-Dox and PEG-GO-Dox are hydrophilic due to the modification with the amine-terminated 6-armed PEG. The presence of PEG minimizes the adsorption of opsonins.<sup>33</sup> As a result, the circulation time of the nanocarrier in blood was enhanced before they reached the targeting sites. No significant difference of the drug distribution in other organs such as the kidney, heart, and lung was observed for different groups ( $p > 0.05$ ).

**Tumor Volume Inhibition and Survival Curves.** The antitumor effect of Dox-loaded nanocarriers in glioma bearing rats was evaluated by tumor volume. After treatment with saline, free Dox, PEG-GO-Dox, and Tf-PEG-GO-Dox, tumor volume at the 14th day of post-intracranial implantation was 326.6, 303.9, 259.7, and 180.8  $\text{mm}^3$ , respectively (Figure S2, Supporting Information). Tf-PEG-GO-Dox exhibited the strongest inhibitory effect on tumor growth compared to other groups ( $p < 0.01$ , Figures 10 and S4, Supporting Information). As TfR is overexpressed on the surface of glioma cells,<sup>9</sup> Tf-PEG-GO-Dox can transport more Dox to the tumor site which has been demonstrated in the tissue distribution assay above and also verified by other studies.<sup>5,12</sup> Tf-PEG-GO-Dox exhibited stronger anticancer effect compared to free Dox or PEG-GO-Dox, as evidenced by the delay of tumor volume expansion. Furthermore, we evaluated the survival curves of brain glioma bearing rats. After treatment with saline, free Dox, PEG-GO-Dox, and Tf-PEG-GO-Dox, the survival range was 11–21, 13–27, 15–28, and 19–34 days, respectively (Figure 11). The rank of median survival time was Tf-PEG-GO-Dox (25 days) > PEG-GO-Dox (21 days) > Dox (19 days) > physiological saline (17 days). By the log-rank test, the median survival time of Tf-PEG-GO-Dox was significantly prolonged compared with that of the saline control, Dox, or PEG-GO-Dox ( $p < 0.05$ ), which reached nearly 41.7%, 31.6%, and 19.0% life-span extension, respectively (Table 1). Taken together, these data demonstrate that Tf-PEG-GO-Dox exhibited the strongest antitumor effect in brain glioma-bearing rats, indicating that Tf conjugated to the surface of PEG-GO can increase the transport of Dox across BBB and reach the glioma.

## CONCLUSIONS

Transferrin conjugated PEGylated GO is explored as an efficient nanovector for targeted delivery of anticancer drugs to brain tumors. Both in vitro and in vivo studies demonstrate that Tf-PEG-GO-Dox is a potential nanoscaled drug delivery system for glioma targeting chemotherapy. Further studies on the mechanism of transmembrane transportation and pharmacokinetics of Tf-GO nanocarrier will help the clinical application of Tf-PEG-GO-Dox in brain tumor treatment.

## ASSOCIATED CONTENT

### Supporting Information

Cytotoxicity of Tf and photographs of the tumor and magnetic resonance (MR) images of tumor volume. This material is available free of charge via the Internet at <http://pubs.acs.org/>.

## ■ AUTHOR INFORMATION

## Corresponding Author

\*Tel: 86-512-67784089 (Q.L.); 86-512-62872556 (Z.Z.). E-mail: lanqingsuzhou@163.com (Q.L.); zjzhang2007@sinano.ac.cn (Z.Z.).

## Author Contributions

#G.L., H.S., and J.M. contributed equally to this work. The manuscript was written through contributions of all authors. All authors have given approval to the final version of the manuscript.

## Notes

The authors declare no competing financial interest.

## ■ ACKNOWLEDGMENTS

This work was supported by University Graduate Students' Scientific Research Innovative Program of Jiangsu Province, China (CX10B-0502) and National Science Foundation of P. R. China (51361130033, 81272799, 81271554, and 21073224).

## ■ REFERENCES

- (1) Behin, A.; Xuan, K. H.; Carpentier, A. F.; Delattre, J. Y. *Lancet* **2003**, *361*, 323–331.
- (2) Allard, E.; Passirani, C.; Garcion, E.; Pigeon, P.; Vessières, A.; Jaouen, G.; Benoit, J. P. *J. Controlled Release* **2008**, *130*, 146–153.
- (3) Partridge, W. M. *Pharm. Res.* **2007**, *24*, 1729–1732.
- (4) Partridge, W. M. *Drug Discovery Today* **2001**, *6*, 381–383.
- (5) Ying, X.; Wen, H.; Lu, W. L.; Du, J.; Guo, J.; Tian, W.; Men, Y.; Zhang, Y.; Li, R. J.; Yang, T. Y.; Shang, D. W.; Lou, J. N.; Zhang, L. R.; Zhang, Q. *J. Controlled Release* **2010**, *141*, 183–192.
- (6) Calvo, P.; Gouritin, B.; Chacun, H.; Desmaële, D.; D'Angelo, J.; Noel, J. P.; Georjgin, D.; Fattal, E.; Andreux, J. P.; Couvreur, P. *Pharm. Res.* **2001**, *18*, 1157–1166.
- (7) Tsutsui, Y.; Tomizawa, K.; Nagita, M.; Michiue, H.; Nishiki, T.; Ohmori, I.; Seno, M.; Matsui, H. *J. Controlled Release* **2007**, *122*, 159–164.
- (8) Jefferies, A. W.; Brandon, M. R.; Hunt, S. V.; Williams, A. F.; Gatter, K. C.; Mason, D. Y. *Nature* **1984**, *312*, 162–163.
- (9) Calzolari, A.; Larocca, L. M.; Deaglio, S.; Finisguerra, V.; Boe, A.; Raggi, C.; Ricci-Itani, L.; Pierconti, F.; Malavasi, F.; De Maria, R.; Testa, U.; Pallini, R. *Transl. Oncol.* **2010**, *3*, 123–134.
- (10) Chang, J.; Paillard, A.; Passirani, C.; Morille, M.; Benoit, J. P.; Betbeder, D.; Garcion, E. *Pharm. Res.* **2012**, *29*, 1495–1505.
- (11) Zhang, P.; Hu, L.; Yin, Q.; Feng, L.; Li, Y. *Mol. Pharm.* **2012**, *9*, 1590–1598.
- (12) Pang, Z.; Gao, H.; Yu, Y.; Guo, L.; Chen, J.; Pan, S.; Ren, J.; Wen, Z.; Jiang, X. *Bioconjugate Chem.* **2011**, *22*, 1171–1180.
- (13) Li, Y.; He, H.; Jia, X.; Lu, W. L.; Lou, J.; Wei, Y. *Biomaterials* **2012**, *33*, 3899–3908.
- (14) Novoselov, K. S.; Geim, A. K.; Morozov, S. V.; Jiang, D.; Zhang, Y.; Dubonos, S. V.; Grigorieva, I. V.; Firsov, A. A. *Science* **2004**, *306*, 666–669.
- (15) Stankovich, S.; Dikin, D. A.; Dommett, G. H.; Kohlhaas, K. M.; Zimney, E. J.; Stach, E. A.; Piner, R. D.; Nguyen, S. T.; Ruoff, R. S. *Nature* **2006**, *442*, 282–286.
- (16) Li, X.; Wang, X.; Zhang, L.; Lee, S.; Dai, H. *Science* **2008**, *319*, 1229–1232.
- (17) Dikin, D. A.; Stankovich, S.; Zimney, E. J.; Piner, R. D.; Dommett, G. H.; Evmenenko, G.; Nguyen, S. T.; Ruoff, R. S. *Nature* **2007**, *448*, 457–460.
- (18) Shen, H.; Zhang, L. M.; Liu, M.; Zhang, Z. J. *Theranostics* **2012**, *2*, 283–294.
- (19) Feng, L. Z.; Liu, Z. *Nanomedicine* **2011**, *6*, 317–324.
- (20) Bao, H.; Pan, Y.; Ping, Y.; Sahoo, N. G.; Wu, T.; Li, L.; Li, J.; Gan, L. H. *Small* **2011**, *7*, 1569–1578.
- (21) Sun, X.; Liu, Z.; Welscher, K.; Robinson, J. T.; Goodwin, A.; Zanic, S.; Dai, H. J. *Nano Res.* **2008**, *13*, 203–212.
- (22) Zhang, L. M.; Xia, J. G.; Zhao, Q. H.; Liu, L. W.; Zhang, Z. J. *Small* **2010**, *6*, 537–544.
- (23) Zhang, W.; Guo, Z.; Huang, D.; Liu, Z.; Guo, X.; Zhong, H. *Biomaterials* **2011**, *32*, 8555–8561.
- (24) Hummers, W. S.; Offeman, R. E. *J. Am. Chem. Soc.* **1958**, *80*, 1339–1339.
- (25) Zhang, L. M.; Wang, Z. L.; Lu, Z. X.; Shen, H.; Huang, J.; Zhao, Q. H.; Liu, M.; He, N. Y.; Zhang, Z. J. *J. Mater. Chem. B* **2013**, *1*, 749–755.
- (26) Pan, H.; Han, L.; Chen, W.; Yao, M.; Lu, W. J. *Controlled Release* **2008**, *125*, 228–235.
- (27) Tian, W.; Ying, X.; Du, J.; Guo, J.; Men, Y.; Zhang, Y.; Li, R.; Yao, H.; Lou, J.; Zhang, L.; Lu, W. L. *Eur. J. Pharm. Sci.* **2010**, *41*, 232–243.
- (28) Yang, K.; Zhang, S.; Zhang, G.; Sun, X.; Lee, S. T.; Liu, Z. *Nano Lett.* **2010**, *10*, 3318–3323.
- (29) Owens, D. E., 3rd.; Peppas, N. A. *Int. J. Pharm.* **2006**, *307*, 93–102.
- (30) Kemper, E. M.; Boogerd, W.; Thuis, I.; Beijnen, J. H.; Tellingena, O. V. *Cancer Treat. Rev.* **2004**, *30*, 415–423.
- (31) Fang, J.; Nakamura, H.; Maeda, H. *Adv. Drug Delivery Rev.* **2011**, *63*, 136–151.
- (32) Schlageter, K. E.; Molnar, P.; Lapin, G. D.; Groothuis, D. R. *Microvasc. Res.* **1999**, *58*, 312–328.
- (33) Schneider, S. W.; Ludwig, T.; Tatenhorst, L.; Braune, S.; Oberleithner, H.; Senner, V.; Paulus, W. *Acta Neuropathol.* **2004**, *107*, 272–276.
- (34) Lotfi, K.; Zackrisson, A. L.; Peterson, C. *Cancer Lett.* **2002**, *178*, 141–149.
- (35) Chang, Y.; Yang, S. T.; Liu, J. H.; Dong, E.; Wang, Y.; Cao, A.; Liu, Y.; Wang, H. *Toxicol. Lett.* **2011**, *200*, 201–210.
- (36) He, H.; Li, Y.; Jia, X. R.; Du, J.; Ying, X.; Lu, W. R.; Lou, J. N.; Wei, Y. *Biomaterials* **2011**, *32*, 478–487.